

Deep Filter Estimation from Inter-Frame Correlations for Monaural Speech Dereverberation

Ui-Hyeop Shin¹, Jun Hyung Kim¹, Jangyeon Kim², Wooseok Kim², Hyung-Min Park^{1,2,*}

¹ Department of Electronic Engineering, Sogang University, Seoul, Republic of Korea

² Department of Artificial Intelligence, Sogang University, Seoul, Republic of Korea

{dmlguql23, imalbert, jykim97, wooseokkim, hpark}@sogang.ac.kr

Abstract

Speech dereverberation in distant-microphone scenarios remains challenging due to the high correlation between reverberation and target signals, often leading to poor generalization in real-world environments. We propose IF-CorrNet, a correlation-to-filter architecture designed for robustness against acoustic variability. Unlike conventional black-box mapping methods that directly estimate complex spectra, IF-CorrNet explicitly exploits inter-frame STFT correlations to estimate multi-frame deep filters for each time-frequency bin. By shifting the learning objective from direct mapping to filter estimation, the network effectively constrains the solution space, which simplifies the training process and mitigates overfitting to synthetic data. Experimental results on the REVERB Challenge dataset demonstrate that IF-CorrNet achieves a substantial gain in the SRMR metric on RealData, confirming its robustness in suppressing reverberation and noise in practical, non-synthetic environments.

Index Terms: multi-frame correlation, multi-frame filtering, speech dereverberation, speech enhancement

1. Introduction

When speech is captured by a distant microphone, reverberation in indoor environments adds long-tail reflections to the direct speech signal, substantially degrading human intelligibility. These reflections smear temporal and spectral details, leading to reduced clarity and increased error rates in downstream tasks. Unlike additive noise, which is usually uncorrelated with the target speech and thus easier to suppress, reverberation remains strongly correlated with the original signal, making it challenging to remove without introducing artifacts or distorting the desired signal.

Although several dereverberation algorithms have been presented based on statistical modeling of target speech [1,2], they have shown limited performance, especially with a single microphone. With the advent of deep learning, a wide range of dereverberation methods have been proposed [3–6], often by treating dereverberation as part of a broader speech enhancement or extraction problem [6–11]. Conventional approaches feed complex STFT components into a network and perform complex masking [3, 12], deep filtering [13, 14], or direct complex spectral mapping [4, 15]. While such methods have shown notable gains, they rely on the model to implicitly disentangle the underlying clean speech from noisy-reverberant raw input signals, often leading to suboptimal convergence behavior by overfitting to training. To alleviate this, two-stage networks have been proposed: the first stage predicts speech components

to estimate inter-frame target and noise covariance matrices, while the second stage estimates multi-frame dereverberation filters [16], yielding improved performance. This is analogous to neural beamforming in the multi-channel case, which estimates beamforming filters from covariance matrices predicted by a separate network [17, 18].

Recently, TF-CorrNet [19] was introduced to exploit spatial information using instantaneous correlations in multi-channel input for joint denoising, dereverberation, and separation. While it demonstrated the structural effectiveness of correlation-based inputs for filter estimation, its reliance on frame-wise spatial correlations limits its application to single-channel scenarios as most common real-world case and results in suboptimal multi-frame filter estimation. To bridge the gap, we propose IF-CorrNet, which explicitly leverages inter-frame correlations as the primary network input. Unlike conventional methods that rely on raw STFT coefficients, IF-CorrNet computes correlations between the current frame and its adjacent frames for each time–frequency bin, directly capturing the physical characteristics of reverberant reflections. By shifting the modeling burden from black-box spectral mapping to explicit filter estimation grounded in inter-frame correlations, our approach naturally preserves the underlying speech structure and significantly enhances robustness against both reverberation and additive noise. For the backbone architecture, we employ dual-path modules [11, 20] to effectively model dependencies across time and frequency sequences derived from these correlation features. Evaluations on the REVERB Challenge [21] dataset demonstrate that our correlation-based filter estimation is superior to conventional methods. Notably, IF-CorrNet maintains consistent and robust performance on real-recorded data (RealData), confirming its effectiveness in modeling complex, non-synthetic reverberation patterns where conventional models often fail to generalize.

2. IF-CorrNet for Speech Dereverberation

Let the observation from a distant microphone be given as $X_{tf} \in \mathbb{C}, 1 \leq t \leq T, 1 \leq f \leq F$ where T and F are the number of time frames and frequency bins, respectively. Then, we can formulate the input observation as

$$X_{tf} = H_f S_{tf} + \sum_{\tau=0}^{L_0} R_{\tau f} S_{t-\tau f} + N_{tf}, \quad (1)$$

where S_{tf} and H_f denote speech source and corresponding direct-path relative transfer function (RTF). On the other hand, $R_{\tau f}$ is convolutive RTF from early reflections and late reverberations. N_{tf} is additive noise. The goal is to obtain the desired direct signal $H_f S_{tf}$ from X_{tf} by suppressing the early reflection, late reverberation, and additive noise.

*indicates the corresponding author.

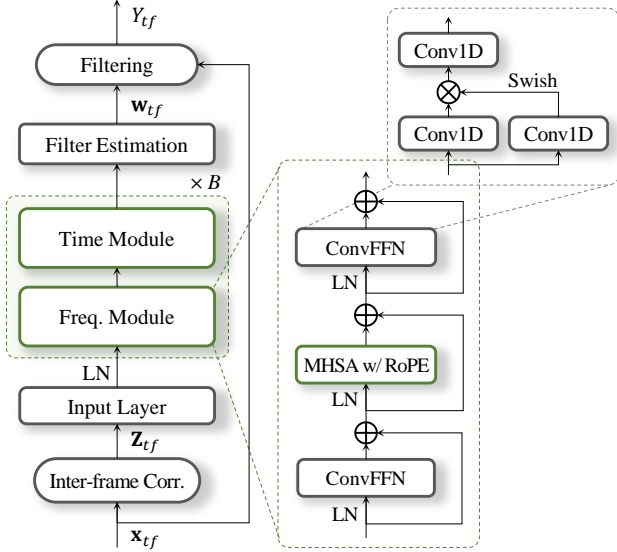


Figure 1: Overall architecture of IF-CorrNet. Inter-frame correlations are processed through input layer, and frequency and time modules to estimate multi-frame filters.

2.1. Inter-frame correlations for deep filter estimation

Building on the formulation in (1), we note that the convolutive RTF terms $R_{\tau f}$ induce strong correlations between the current frame X_{tf} and both its past frames $X_{t-\tau f}$ and future frames $X_{t+\tau f}$. By explicitly computing these inter-frame correlations—rather than feeding single frame complex STFT coefficients—our model receives a direct cue of the reverberant structure imposed by $R_{\tau f}$, enabling more accurate dereverberation filter estimation.

Specifically, let $\mathbf{x}_{tf} = [X_{(t-L)f}, \dots, X_{tf}, \dots, X_{(t+L)f}]^T \in \mathbb{C}^{2L+1}$ be the multi-frame observations where $2L + 1$ is the number of taps. Instead of directly using the components of the STFT X_{tf} , the network input can be given by inter-frame correlations $\mathbf{Z}_{tf} \in \mathbb{C}^{(2L+1) \times (2L+1)}$ as

$$\mathbf{Z}_{tf} = \mathbf{x}_{tf} \mathbf{x}_{tf}^H. \quad (2)$$

as shown in Figure 1. In the inter-frame correlation matrix \mathbf{Z}_{tf} , magnitude components are naturally included, which is known to be helpful for speech enhancement and separation [10, 22]. On the other hand, power scales of correlations can lead to unstable training. Therefore, when denoting that $[\mathbf{Z}_{tf}]_{m,n} = X_{(t-L+m)f} X_{(t-L+n)f}^*$, $0 \leq m, n \leq 2L$, we utilize generalized PHAT- β [19, 23] weighting as

$$[\mathbf{Z}_{tf}]_{m,n} \leftarrow \frac{X_{(t-L+m)f} X_{(t-L+n)f}^*}{|X_{(t-L+m)f} X_{(t-L+n)f}^*|^\beta}, \quad (3)$$

where $0 \leq \beta \leq 1$. In this paper, we set β to 0.5 for simplicity.

Then, these correlations are processed by the network to estimate the same length of deep filter $\mathbf{w}_{tf} \in \mathbb{C}^{2L+1}$ at each time-frequency bin. Then, the output can be calculated as

$$Y_{tf} = \mathbf{w}_{tf}^T \mathbf{x}_{tf}. \quad (4)$$

2.2. Time-frequency module

As an input feature for the network, the inter-frame correlations \mathbf{Z}_{tf} are flattened and their real and imaginary components are

concatenated for the network input, which makes input tensors of shape $\mathbb{R}^{2(2L+1)^2 \times T \times F}$. As shown in Figure 1, the flattened correlations are encoded into an input feature of shape $\mathbb{R}^{C \times T \times F}$ by the input layer. The input layer consists of two 2D convolution layers (Conv2D) with kernel sizes of (1,1) and (3,3), and output channels of $2C$ and C , respectively. We use the SwiGLU function as the intermediate activation, where the gating function is swish. This is followed by layer normalization (LN). Unlike the former approaches based on spectral mapping [10, 11] using global layer normalization (gLN) [24], we used LN applied to each time-frequency bin, which is empirically effective for filter estimation structure and improved robustness.

The time-frequency features are then processed B times through frequency and time modules based on a modified Transformer to improve local context modeling [11]. In the frequency module, the features are treated as T independent sequences of length F , with shape $\mathbb{R}^{T \times F \times C}$, to capture inter-frequency dependencies. In the time module, the features are instead treated as F independent sequences of length T . The temporal module allows the network to learn inter-frame correlations within the same frequency bin. Finally, the processed features are projected by a Conv2D layer with kernel size (1,1) and reshaped into $\mathbb{R}^{2(2L+1) \times T \times F}$ to estimate the output filter \mathbf{w}_{tf} .

2.3. Transformer block with ConvFFN module

For speech processing, local context plays a critical role. However, it is often challenging for the multi-head self-attention (MHSA) to consistently maintain locally smooth attention weights. Therefore, because designing a model having a strong local-modeling capability should be considered, we adopt the macaron-style Transformer [25] blocks with two convolution-augmented FFN (ConvFFN) inspired by TF-LoCoformer [11]. Along with MHSA with rotational positional encoding (RoPE) [26], two ConvFFN modules are placed as illustrated in Figure 1. Unlike the vanilla FFN, which consists of two linear layers, or equivalently point-wise convolution, ConvFFN modules are based on two 1D convolution layers to model the local time-frequency contexts with hidden dimension. We also utilize SwiGLU as hidden activation in ConvFFN layer.

3. Experimental Setups

3.1. Datasets and evaluation

We conducted experiments on the REVERB Challenge corpus [21], which provides both simulated and real recordings sampled at 16 kHz. The corpus is divided into training, development, and evaluation subsets with no speaker overlap across them. The training set comprises 7,861 clean utterances from the WSJ0 database. Reverberant training examples were generated by convolving these clean signals with 24 measured room impulse responses covering reverberation times (T60) from 0.2 s to 0.8 s, followed by the addition of diffuse background noise at SNR of 20 dB. For fair comparison, we trained the proposed models only on these simulated mixtures without applying further data augmentation [16].

The development and evaluation sets include both simulated (“SimData”) and real (“RealData”) recordings. This design allows assessment under controlled reverberant conditions as well as in real acoustic environments with additional mismatches. The SimData set contains 1,484 utterances for development and 2,176 for evaluation, derived from the WSJ-CAM0 corpus [27]. These signals were processed with im-

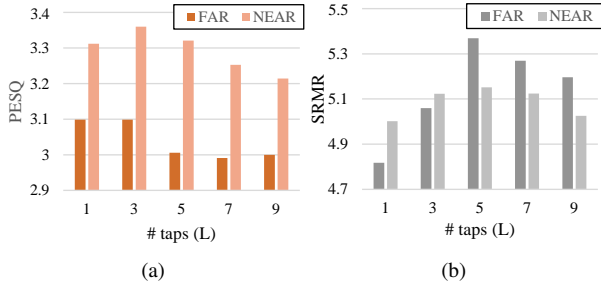


Figure 2: Plot of (a) PESQ and (b) SRMR results on REVERB Challenge dataset depending on the number of taps L .

pulse responses measured in three rooms of different sizes (small, medium, and large) at near and far microphone distances, and mixed with stationary low-frequency noise dominated by air-conditioning hum. In contrast, the RealData set consists of 179 development and 372 evaluation utterances recorded in a physical room not included in the simulated data, with source–microphone distances of 1 m and 2.5 m, providing a more challenging generalization scenario.

All models were trained on the simulated training set, and the best system was selected using SimData from the development set. Final evaluation was conducted on the SimData and RealData evaluation set. Performance was measured using the objective metrics defined in the REVERB Challenge, including (i) cepstral distance (CD), (ii) log-likelihood ratio (LLR), (iii) frequency-weighted segmental SNR (SNR_{fw}), (iv) perceptual quality (PESQ), and (v) signal-to-reverberation modulation energy ratio (SRMR). Since most metrics require paired clean references, they were computed only for SimData, whereas SRMR was additionally applied to RealData to quantify dereverberation performance in mismatched conditions.

3.2. Training and model configuration

All models were trained using the AdamW optimizer for maximum 40 epochs. The models were trained using 4-second segments with a batch size of 2. STFT was computed using a Hanning window of size 512 and a hop size of 256. For the IF-CorrNet, B and C were set to 6 and 96. A hidden dimension C_H and a kernel size K are set to 192 and 7 in the ConvFFN module, respectively. We additionally trained small version of IF-CorrNet with $C = 64$, $B = 6$, $C_H = 128$, $K = 3$. The number of heads in MHSA is commonly 4. For training loss, time-domain L_1 loss and TF-domain multi-resolution L_1 loss [28] were utilized, in which we used four FFT window sizes {256, 512, 768, 1024}. For pair comparison, we followed the same training procedure as in [16].

4. Experimental Results

4.1. Investigation on the number of taps

First, we evaluated IF-CorrNet with respect to the number of taps L to determine an appropriate temporal context for deep filter estimation. Figure 2 reports PESQ and SRMR on SimData under near- and far-microphone conditions. PESQ peaks at $L = 3$ and gradually decreases for larger L . Since PESQ is sensitive to speech distortion, this indicates that while longer filters suppress reverberation more aggressively, excessively large L can distort correlated speech components.

In contrast, SRMR increases more consistently with L and

Table 1: Performance comparison of existing methods on the REVERB Challenge test set.

Method	SimData					RealData
	CD $^\downarrow$	SRMR $^\uparrow$	LLR $^\downarrow$	SNR $_{fw}^\uparrow$	PESQ $^\uparrow$	SRMR $^\uparrow$
No Processing	3.975	3.687	0.574	3.617	1.503	3.180
WPE [29]	3.748	4.220	0.514	4.864	1.722	3.978
WRN [30]	3.590	3.590	0.470	4.800	-	3.240
GCRN [31]	2.534	4.861	0.325	10.753	1.934	4.846
TCN+SA [32]	2.200	5.170	0.240	13.060	2.580	5.540
D-MFMVDR [33]	2.639	4.892	0.316	9.649	2.167	5.530
DCN [16]	2.001	5.269	0.225	13.326	2.935	6.476
IF-CorrNet(<i>small</i>)	2.359	4.966	0.233	14.295	3.016	7.009
IF-CorrNet	1.899	5.091	0.179	15.663	3.230	7.548

Table 2: Comparison of computational complexity and performance against high-performing backbones.

Method	Param (M)	MAC (G)	RTF	SimData		RealData
				SNR $_{fw}^\uparrow$	PESQ $^\uparrow$	SRMR $^\uparrow$
No Processing	-	-	-	3.617	1.503	3.180
TF-GridNet	8.4	127.3	0.081	14.458	2.825	7.319
MP-SENet	2.3	22.2	0.022	13.622	2.811	7.007
TF-Loformer	15.0	258.2	0.028	14.102	2.642	6.639
IF-CorrNet(<i>small</i>)	2.1	33.7	0.024	14.295	3.016	7.009
IF-CorrNet	10.0	161.4	0.025	15.663	3.230	7.548

reaches a peak around $L = 5$, suggesting that longer temporal context better captures long-tail reverberation. The far-field condition, which is more severely reverberant, benefits more from increasing L and eventually surpasses the near-field SRMR. This crossover implies that, given sufficient temporal context, the proposed correlation-to-filter formulation can better exploit inter-frame structures in far-field recordings.

Overall, the results reveal a trade-off between dereverberation strength (SRMR) and speech distortion sensitivity (PESQ). Considering both metrics and stability across microphone distances, we adopt $L = 3$ as the baseline configuration in the remaining experiments.

4.2. Comparison with existing baselines

We first compare IF-CorrNet with representative single-channel dereverberation baselines on the REVERB Challenge dataset: WPE [29], WRN [30], GCRN [31], TCN+SA [32], D-MFMVDR [33], and DCN [16]. Table 1 summarizes results on the SimData and RealData evaluation sets. Overall, IF-CorrNet achieves the best performance on SimData across CD/LLR/SNR $_{fw}$ /PESQ, while also providing a substantial SRMR gain on RealData. Notably, IF-CorrNet(*small*) still improves RealData SRMR (7.009) and remains competitive on SimData, indicating that the proposed formulation is effective even under constrained model capacity.

4.3. Efficiency and distance robustness analysis

Beyond Table 1, we conduct a controlled comparison against recent high-performing enhancement backbones (TF-GridNet [10], MP-SENet [34], and TF-Loformer [11]) trained under the same REVERB protocol. For mapping-based

Table 3: Performance comparison across microphone distances and analysis of distance sensitivity on SimData.

Method	PESQ			SNR _{fw}		
	Far	Near	Diff.(Δ)	Far	Near	Diff.(Δ)
No Processing	1.339	1.667	0.328	2.650	4.582	1.932
DCN [16]	2.553	3.317	0.764	12.280	14.371	2.091
TF-GridNet	2.503	3.149	0.646	13.003	15.913	2.910
MP-SENet	2.566	3.056	0.490	12.414	14.829	2.415
TF-LoCoformer	2.385	2.900	0.515	12.542	15.663	3.121
IF-CorrNet(<i>small</i>)	2.861	3.170	0.309	13.020	15.570	2.550
IF-CorrNet	3.099	3.360	0.261	14.543	16.783	2.240

Table 4: Ablation study results on the REVERB Challenge evaluation set (SimData). SF and MF denotes single-frame and multi-frame respectively.

Input	Output	SimData				RealData	
		CD [↓]	SRMR [↑]	LLR [↓]	SNR _{fw} [↑]	PESQ [↑]	SRMR [↑]
IF-Corr.	MF-Filter	1.899	5.091	0.179	15.663	3.230	7.548
SF-Raw	MF-Filter	2.003	5.022	0.191	15.471	3.246	7.225
SF-Raw	SF-Mask	2.006	5.011	0.198	15.453	3.244	7.245
SF-Raw	Mapping	2.891	4.924	0.336	11.657	2.710	6.628

baselines, input normalization and inverse rescaling are applied for optimal results. Table 2 reports performance together with model complexity (parameters, MACs) and runtime (RTF) measured on Nvidia GeForce RTX 5090.

While TF-GridNet performs strongly, its inference speed is severely bottlenecked with a Real-Time Factor (RTF) of 0.081, making it about three times slower than other methods. Furthermore, TF-LoCoformer demands substantial computational resources, yet struggles to generalize to real-world environments, yielding a lower RealData SRMR. In contrast, IF-CorrNet achieves the best overall scores while maintaining a highly efficient inference speed (RTF 0.025). Moreover, IF-CorrNet(*small*) proves the structural advantage of explicitly exploiting inter-frame correlations with small model size and computations, it delivers competitive performance and surpasses heavier baselines in practical generalization at a runtime comparable to lightweight models like MP-SENet.

To further examine robustness across microphone distances, Table 3 reports far- and near-field results on SimData. IF-CorrNet achieves the strongest far-field performance and shows the smallest PESQ distance gap, with a near-minimal SNR_{fw} gap, indicating reduced sensitivity to source-microphone distance. These results are consistent with our motivation that explicitly modeling inter-frame correlations improves robustness in distant-microphone scenarios.

4.4. Impact of Inter-frame correlations on robustness

To analyze the contribution of each key component in our proposed IF-CorrNet, we conducted an ablation study. We focused on validating two primary architectural choices: the inter-frame correlation (IF-Corr.) input feature and the multi-frame filtering (MF-Filter) output mechanism. The results are summarized in Table 4. We evaluated the following four model configurations:

- IF-Corr. + MF-Filter: The proposed model utilizing inter-

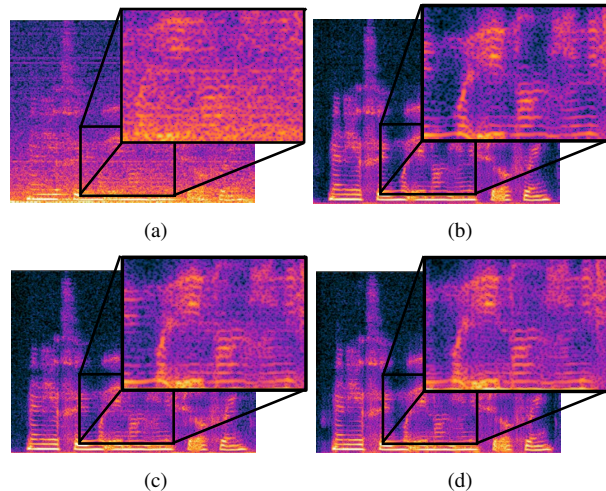


Figure 3: Spectrogram of sample utterance of RealData on REVERB Challenge Dataset: (a) Input and output from (b) IF-Corr + MF-Filter, (c) SF-Raw + MF-Filter, and (d) SF-Raw + SF-Mask.

frame correlation input and multi-frame filtering output.

- SF-Raw + MF-Filter: The inter-frame correlation input is replaced with a single-frame raw STFT input.
- SF-Raw + SF-Mask: The output is estimated by a single-frame complex masking in addition to the raw STFT.
- SF-Raw + Mapping: model is modified to perform direct spectral mapping.

Table 4 shows that replacing IF-Corr. with raw single-frame STFT degrades CD/LLR/SNR_{fw} on SimData and reduces RealData SRMR, highlighting that correlation features are the primary driver of robustness under acoustic mismatch. With SF-Raw input, MF-Filter and SF-Mask perform similarly, suggesting that increasing temporal context in the *output* alone provides limited benefit when the input does not explicitly expose inter-frame structure. Direct spectral mapping yields the worst results, consistent with its higher susceptibility to overfitting on simulated training conditions.

Figure 3 further illustrates a RealData example, where the proposed correlation-to-filter estimation produces the cleanest dereverberated spectrogram. A demo page is available¹.

5. Conclusion

In this work, we introduced IF-CorrNet, a deep filter estimation model for monaural speech dereverberation that explicitly leverages inter-frame correlations rather than raw complex STFT inputs. By exploiting correlations between adjacent time frames as the primary network input, IF-CorrNet effectively estimates multi-frame dereverberation filters. Experimental evaluation on the REVERB Challenge corpus demonstrated that IF-CorrNet achieves superior performance compared to conventional baselines, consistently improving dereverberation quality especially for real-recorded conditions.

Future work includes further exploration of inter-frame correlations and extension to multi-channel scenarios by incorporating spatio-temporal correlations, and to more comprehensive tasks including denoising, dereverberation, and separation.

¹https://ifcornet.github.io/IF_CorrNet_demo/

6. Generative AI Use Disclosure

Generative AI tools were used solely for editing and polishing the manuscript to improve linguistic clarity. These tools were not employed to produce any significant portion of the technical or scientific content, and the authors remain fully responsible and accountable for the integrity and final results of the work.

7. References

- [1] T. Nakatani, T. Yoshioka, K. Kinoshita, M. Miyoshi, and B.-H. Juang, "Speech Dereverberation Based on Variance-Normalized Delayed Linear Prediction," *IEEE Transactions on Audio, Speech, and Language Processing*, vol. 18, no. 7, pp. 1717–1731, 2010.
- [2] T. Yoshioka and T. Nakatani, "Generalization of Multi-Channel Linear Prediction Methods for Blind MIMO Impulse Response Shortening," *IEEE Transactions on Audio, Speech, and Language Processing*, vol. 20, no. 10, pp. 2707–2720, 2012.
- [3] O. Ernst, S. E. Chazan, S. Gannot, and J. Goldberger, "Speech Dereverberation Using Fully Convolutional Networks," in *2018 26th European Signal Processing Conference (EUSIPCO)*, 2018, pp. 390–394.
- [4] Z.-Q. Wang and D. Wang, "Deep Learning Based Target Cancellation for Speech Dereverberation," *IEEE/ACM Transactions on Audio, Speech, and Language Processing*, vol. 28, pp. 941–950, 2020.
- [5] —, "Multi-Microphone Complex Spectral Mapping for Speech Dereverberation," in *Proc. IEEE Int. Conf. Acoust., Speech Signal Process. (ICASSP)*, 2020, pp. 486–490.
- [6] T. Lavanya, T. Nagarajan, and P. Vijayalakshmi, "Multi-Level Single-Channel Speech Enhancement Using a Unified Framework for Estimating Magnitude and Phase Spectra," *IEEE/ACM Transactions on Audio, Speech, and Language Processing*, vol. 28, pp. 1315–1327, 2020.
- [7] D. S. Williamson and D. Wang, "Time-Frequency Masking in the Complex Domain for Speech Dereverberation and Denoising," *IEEE/ACM Transactions on Audio, Speech, and Language Processing*, vol. 25, no. 7, pp. 1492–1501, 2017.
- [8] C. S. J. Doire, M. Brookes, P. A. Naylor, C. M. Hicks, D. Betts, M. A. Dmour, and S. H. Jensen, "Single-Channel Online Enhancement of Speech Corrupted by Reverberation and Noise," *IEEE/ACM Transactions on Audio, Speech, and Language Processing*, vol. 25, no. 3, pp. 572–587, 2017.
- [9] Y. Zhao, Z.-Q. Wang, and D. Wang, "Two-Stage Deep Learning for Noisy-Reverberant Speech Enhancement," *IEEE/ACM Transactions on Audio, Speech, and Language Processing*, vol. 27, no. 1, pp. 53–62, 2019.
- [10] Z.-Q. Wang, S. Cornell, S. Choi, Y. Lee, B.-Y. Kim, and S. Watanabe, "TF-GridNet: Integrating Full- and Sub-Band Modeling for Speech Separation," *IEEE/ACM Transactions on Audio, Speech, and Language Processing*, vol. 31, pp. 3221–3236, 2023.
- [11] K. Saijo, G. Wichern, F. G. Germain, Z. Pan, and J. L. Roux, "TF-LoCoformer: Transformer with Local Modeling by Convolution for Speech Separation and Enhancement," in *2024 18th International Workshop on Acoustic Signal Enhancement (IWAENC)*, 2024, pp. 205–209.
- [12] Y. Hu, Y. Liu, S. Lv, M. Xing, S. Zhang, Y. Fu, J. Wu, B. Zhang, and L. Xie, "DCCRN: Deep Complex Convolution Recurrent Network for Phase-Aware Speech Enhancement," in *Proc. Interspeech*, 2020, pp. 2472–2476.
- [13] W. Mack and E. A. P. Habets, "Deep Filtering: Signal Extraction and Reconstruction Using Complex Time-Frequency Filters," *IEEE Signal Processing Letters*, vol. 27, pp. 61–65, 2020.
- [14] H. Schroter, A. N. Escalante-B, T. Rosenkranz, and A. Maier, "Deepfilternet: A Low Complexity Speech Enhancement Framework for Full-Band Audio Based On Deep Filtering," in *Proc. IEEE Int. Conf. Acoust., Speech Signal Process. (ICASSP)*, 2022, pp. 7407–7411.
- [15] K. Tan and D. Wang, "Complex Spectral Mapping with a Convolutional Recurrent Network for Monaural Speech Enhancement," in *Proc. IEEE Int. Conf. Acoust., Speech Signal Process. (ICASSP)*, 2019, pp. 6865–6869.
- [16] V. Kothapally and J. H. L. Hansen, "Monaural Speech Dereverberation Using Deformable Convolutional Networks," *IEEE/ACM Transactions on Audio, Speech, and Language Processing*, vol. 32, pp. 1712–1723, 2024.
- [17] Z. Zhang, Y. Xu, M. Yu, S.-X. Zhang, L. Chen, and D. Yu, "ADL-MVDR: All Deep Learning MVDR Beamformer for Target Speech Separation," in *Proc. IEEE Int. Conf. Acoust., Speech Signal Process. (ICASSP)*, 2021, pp. 6089–6093.
- [18] Z. Zhang, T. Yoshioka, N. Kanda, Z. Chen, X. Wang, D. Wang, and S. E. Eskimez, "All-Neural Beamformer for Continuous Speech Separation," in *Proc. IEEE Int. Conf. Acoust., Speech Signal Process. (ICASSP)*, 2022, pp. 6032–6036.
- [19] U.-H. Shin, B. H. Ku, and H.-M. Park, "TF-CorrNet: Leveraging Spatial Correlation for Continuous Speech Separation," *IEEE Signal Processing Letters*, vol. 32, pp. 1875–1879, 2025.
- [20] F. Dang, H. Chen, and P. Zhang, "DPT-FSNet: Dual-Path Transformer Based Full-Band and Sub-Band Fusion Network for Speech Enhancement," in *Proc. IEEE Int. Conf. Acoust., Speech Signal Process. (ICASSP)*, 2022, pp. 6857–6861.
- [21] K. Kinoshita, M. Delcroix, T. Yoshioka, T. Nakatani, E. Habets, R. Haeb-Umbach, V. Leutnant, A. Sehr, W. Kellermann, R. Maas, S. Gannot, and B. Raj, "The rever challenge: A common evaluation framework for dereverberation and recognition of reverberant speech," in *2013 IEEE Workshop on Applications of Signal Processing to Audio and Acoustics*, 2013, pp. 1–4.
- [22] R. Cao, S. Abdulatif, and B. Yang, "CMGAN: Conformer-based Metric GAN for Speech Enhancement," in *Proc. Interspeech*, 2022, pp. 936–940.
- [23] K. D. Donohue, J. Hannemann, and H. G. Dietz, "Performance of phase transform for detecting sound sources with microphone arrays in reverberant and noisy environments," *Signal Processing*, vol. 87, no. 7, pp. 1677–1691, 2007.
- [24] Y. Luo and N. Mesgarani, "Conv-TasNet: Surpassing Ideal Time-Frequency Magnitude Masking for Speech Separation," *IEEE/ACM Trans. Audio, Speech, Language Process.*, vol. 27, no. 8, pp. 1256–1266, 2019.
- [25] Y. Lu*, Z. Li*, D. He, Z. Sun, B. Dong, T. Qin, L. Wang, and T. yan Liu, "Understanding and Improving Transformer From a Multi-Particle Dynamic System Point of View," in *ICLR 2020 Workshop on Integration of Deep Neural Models and Differential Equations*, 2019.
- [26] J. Su, M. Ahmed, Y. Lu, S. Pan, W. Bo, and Y. Liu, "RoFormer: Enhanced transformer with Rotary Position Embedding," *Neurocomputing*, vol. 568, p. 127063, 2024.
- [27] T. Robinson, J. Franssen, D. Pye, J. Foote, and S. Renals, "WSJ-CAMO: a British English speech corpus for large vocabulary continuous speech recognition," in *1995 International Conference on Acoustics, Speech, and Signal Processing*, vol. 1, 1995, pp. 81–84 vol.1.
- [28] Y.-J. Lu, S. Cornell, X. Chang, W. Zhang, C. Li, Z. Ni, Z.-Q. Wang, and S. Watanabe, "Towards Low-Distortion Multi-Channel Speech Enhancement: The ESPNET-SE Submission to the L3DAS22 Challenge," in *Proc. IEEE Int. Conf. Acoust., Speech Signal Process. (ICASSP)*, 2022, pp. 9201–9205.
- [29] T. Yoshioka and T. Nakatani, "Generalization of Multi-Channel Linear Prediction Methods for Blind MIMO Impulse Response Shortening," *IEEE Transactions on Audio, Speech, and Language Processing*, vol. 20, no. 10, pp. 2707–2720, 2012.
- [30] J. Llombart, D. Ribas, A. Miguel, L. Vicente, A. Ortega, and E. Lleida, "Speech Enhancement with Wide Residual Networks in Reverberant Environments," in *Interspeech 2019*, 2019, pp. 1811–1815.

- [31] O. Hazrati, S. Sadjadi, P. Loizou, and J. Hansen, "Simultaneous suppression of noise and reverberation in cochlear implants using a ratio masking strategy," *The Journal of the Acoustical Society of America*, vol. 134, pp. 3759–65, 11 2013.
- [32] H. Wang, Y. Wang, Q. Zhang, S. Xiang, and C. Pan, "Gated Convolutional Neural Network for Semantic Segmentation in High-Resolution Images," *Remote Sensing*, vol. 9, no. 5, 2017.
- [33] Z. Zhang, Y. Xu, M. Yu, S.-X. Zhang, L. Chen, D. S. Williamson, and D. Yu, "Multi-Channel Multi-Frame ADL-MVDR for Target Speech Separation," *IEEE/ACM Transactions on Audio, Speech, and Language Processing*, vol. 29, pp. 3526–3540, 2021.
- [34] Y.-X. Lu, Y. Ai, and Z.-H. Ling, "MP-SENet: A Speech Enhancement Model with Parallel Denoising of Magnitude and Phase Spectra," in *Proc. Interspeech*, 2023, pp. 3834–3838.